

THE UNIVERSITY OF CHICAGO

SPATIOTEMPORAL CORRELATION TRANSFER IN PLASTIC  
EXCITATORY-INHIBITORY NEURONAL NETWORKS

A THESIS SUBMITTED TO  
THE FACULTY OF THE DIVISION OF THE PHYSICAL AND BIOLOGICAL  
SCIENCES  
IN CANDIDACY FOR THE DEGREE OF  
MASTER OF SCIENCE  
GRADUATE PROGRAM IN BIOPHYSICS

BY  
CLAYTON W. SEITZ

CHICAGO, ILLINOIS  
WINTER 2021

Copyright © 2021 by Clayton W. Seitz  
All Rights Reserved

## Epigraph

# TABLE OF CONTENTS

ACKNOWLEDGMENTS . . . . .	v
ABSTRACT . . . . .	vi
1 SPATIOTEMPORAL CORRELATION TRANSFER IN PLASTIC EXCITATORY- INHIBITORY NEURONAL NETWORKS . . . . .	1
1.1 Introduction . . . . .	1
1.2 Literature Review . . . . .	5
1.2.1 The diffusion approximation . . . . .	6
1.2.2 Beyond the diffusion approximation . . . . .	13
1.2.3 Reshaping network structure with synaptic plasticity . . . . .	15
1.2.4 Reflecting on the interpretation of network dynamics . . . . .	25
1.3 Results . . . . .	26
1.3.1 The two-dimensional Gaussian network . . . . .	26
1.3.2 Homogeneous Gaussian networks . . . . .	31
1.3.3 Excitatory-inhibitory Gaussian networks . . . . .	33
1.4 Methods . . . . .	36
1.4.1 Signal processing techniques . . . . .	36
APPENDICES . . . . .	39
REFERENCES . . . . .	40

## ACKNOWLEDGMENTS

# ABSTRACT

A central goal in computational neuroscience is to explain how functional brain states emerge from the complex interactions of excitatory and inhibitory neurons in specialized brain regions and the subnetworks within them. Recent years have hosted many efforts to decode the complex patterns of action potentials in response to sensory stimuli by examining the cross-covariance of neural spike trains. The dynamics of complex networks in the brain is determined by many factors including network topology, synaptic plasticity, homeostatic changes and noise. Synaptic plasticity is of considerable interest as it allows neural circuits to guide their own topological evolution and adapt to externally and internally generated brain states. An important tool in this pursuit is the recurrent spiking neural network (RSNN) model which allows us to explore the structural properties of plastic excitatory-inhibitory networks and the relationship of structure to correlated dynamics. Recently, a number of mathematical tools for understanding spike train cross-covariance based on mean-field theory and linear response theory have emerged. The application of these tools to plastic networks of neurons holds great promise for improving our understanding of functional brain states and the principles of neural computation. However, our understanding of the structural origins of correlated dynamics in response to temporally correlated stimuli is lacking. In this thesis, I propose an extension of existing theoretical models of spike-train cross-covariance for plastic excitatory-inhibitory networks. This extension serves to improve our understanding of the structural basis of spike-train cross-covariance and the structural and response dynamics of neural circuits for temporally correlated stimuli.

# CHAPTER 1

## SPATIOTEMPORAL CORRELATION TRANSFER IN PLASTIC EXCITATORY-INHIBITORY NEURONAL NETWORKS

### 1.1 Introduction

Complex systems are ubiquitous in nature yet our scientific efforts have thus far only begun to gain traction on their governing principles. Many of the most intriguing complex systems in nature exhibit behaviors that simply cannot be explained by any of the components in isolation but rather arise from their interactions, bringing emergent phenomena into the focus of modern science. The human brain exemplifies this complexity, thought to consist of billions of noisy neurons, yet the dynamics of these neurons simultaneously maintain an order evident in the stability of our sensory percepts.

It is well accepted that information processing in the brain like sensory, motor, and cognitive functions are carried out by the communication between individual neurons, formally referred to as a *population code*. Amongst a wide variety of cell types, the dominating information processing unit in neocortex is the spiking neuron - a cell which exhibits transient depolarization and repolarization of the plasma membrane called action potentials or *spikes*. Neurons in cortex connect when afferent nerve fibers of one cell meet the dendritic tree or soma of another, forming the synapse. The complexity of the structure of neural networks therefore arises from the complex wiring of these communication channels. It is a great challenge to understand how connectivity patterns in cortex interact with sensory stimuli via synaptic transmission to give rise to conscious experience.

In his famous neurophysiological postulate, Donald Hebb first proposed a cellular mechanism for the self-organization of networks of neurons. Hebb suggested that repeated stimulation of specific receptors of sensory signals would lead slowly to the formation of a *cell*

*assembly* and these structural changes would constitute a representation or imprint of an internally or externally generated sensation e.g., an image or idea [1]. This process, referred to as Hebbian learning, is argued to be driven by the temporal order of action potentials where the efficacy of transmission across a synapse can be modified according to sensory experience. Our understanding of these mechanisms from a neurobiological point view has drastically improved since this idea was first presented. However, phenomena which are thought to rely on changes in synaptic wiring, such as memory formation, still have yet to be fully explained from first principles.

The computations carried out by cortical circuits cannot depend on synaptic wiring alone, but are likely to depend on a complex interaction of network architecture and externally and internally generated stimuli. Thus a

Simultaneously, a host of plasticity mechanisms are constantly molding the network topology. Furthermore, it stands to reason that the population code employed by cortical circuits will become evident after suitable analysis of the correlation structure of neural spike trains.

On the other hand, *in-vivo*, spike-train correlations resulting from overlapping synaptic inputs must be distinguished from correlations which arise from environmental factors outside a controlled stimulus. Often referred to as noise correlations, these correlations cannot be reproduced across experimental trials and are closely linked to the trial-to-trial variability observed experimentally. The role of noise correlations in the brain is poorly understood, although it is widely regarded to contribute to the amount of information that can be encoded by a neuronal population (Cohen 2011). In principle, stochasticity can be introduced into a system of neurons in a few different ways: (i) by intrinsic noise - the noise introduced into the system by the random interactions of a cell's molecular components at nonzero temperature (ii) background activity i.e., afferent synaptic inputs that are not members of the population being simulated or recorded (iii) by stochastic features of the stimulus used to generate



network activity. If the system is assumed to be closed (as in a computer simulation), the only possible noise sources come from (i) and (iii). Therefore, in the remainder of the text, we assume that the only contributing factors to spike-train correlations are overlapping synaptic input pools and that any noise that is intrinsic to any one neuron is uncorrelated with that of all other neurons in the population.

An ideal theory of cortical dynamics would be able to precisely predict the future state of the state variables of each individual neuron, e.g. the membrane potential, given their current state. However, stochastic features of single neuron dynamics make such a theory intractable. Accordingly, some of the most mature models of cortical dynamics owe their origins to statistical physics. It is common in statistical physics to be faced with a very high-dimensional system whose microscopic dynamics cannot be predicted exactly. One solution to this problem is to develop a so-called mean field theory (MFT), where the interactions between individual units are replaced by their average values. While an approximation, this solution has had success in predicting the average dynamics of networks in the limit of very large numbers of neurons. Another approach is to develop an ensemble density model, where, under the appropriate assumptions, the probability density of neuron state variables and its dependence on time can be predicted analytically (Brunel 2000). Such models often rely on a diffusion approximation of the Kramers-Moyal expansion, which therefore involves the solution of a second-order differential equation for the population density of a state variable as a function of time. These equations are notoriously difficult to solve, although in a few special cases, a solution can be found.

Moreover, early models of cortical computation were deterministic and therefore assumed cortical computations are carried out in a logical fashion. However, an increasing body of experimental data suggests that neurons, synapses, and systems of neurons are inherently stochastic (Buesing, 2011). The enormous number of degrees of freedom of just a single cell due to millions of unreliable ion channels and synaptic machinery demands a stochastic

model for network dynamics (Cannon, 2010; Tuckwell, 1989). Indeed, it has been argued that the trial-to-trial variability in neural responses to stimuli and the irregularity of spike-timing owe their origins to noise in the synaptic integration process (Azouz, 1999). Importantly, *noise* here refers to unpredictable features of synaptic integration by the postsynaptic cell and not to the presynaptic spikes themselves.

The apparent reliability of cortical computations at the scale of networks suggests that the brain has evolved to accommodate for synaptic noise or perhaps even incorporated the noise into its computational paradigm (Rolls, 2010). In recent decades, a great deal of effort has been spent investigating the hypothesis that networks of neurons perform sensory processing via probabilistic, rather than logical inference. Probabilistic inference is a rich mathematical framework that has experienced success in fields such as machine learning and artificial intelligence and, more recently, computational neuroscience. These ideas have been recently applied in a variety of subdomains including sensorimotor learning (Kording, 2004), object recognition (Kersten 2004), visual processing (Lee 2003), and perceptual multistability (Sundareswara 2008). In the probabilistic framework, neural responses to stimuli are viewed as sampling from a posterior distribution, conditioned on the stimulus (Hoyer 2002; Buesing 2011). This framework naturally accommodates for the stochastic effects introduced by the biological substrate. At the same time, a stochastic description of network dynamics does not exclude a rigorous understanding of the transmission of information. Quite the contrary, information transmission in single neurons can be quantified precisely via the use of Shannon’s information theory (MacKay, McCulloch 1952). More recently, this theory has been applied in the quantification of how much information flows through the nervous system, and the constraints that information theory imposes on the capabilities of neural systems for communication, computation and behavior (Dimitrov 2011).

Most recently, artificial spiking neural networks (SNNs) have been developed that strive to replicate human cognitive capabilities such as language processing or temporal credit

assignment (Bellec 2020). Such networks incorporate biologically plausible online learning rules thought to be similar to those employed by the brain. Nevertheless, these models are highly task-oriented and therefore difficult to apply to other tasks or sensory processing at large. Therefore, here we consider the dynamics of a spiking neural network stimulated with a multivariate gaussian signal with well-defined covariance.

## 1.2 Literature Review

A central goal of modern neuroscience is to explain how functional brain states emerge from the interactions of dozens, perhaps hundreds, of brain regions, each containing its own complex subnetworks. These subnetworks can themselves contain thousands of cells, each neuron having on the order of thousands of synaptic connections to other cells within the local network (Binzegger 2004). In fact, connection probabilities between nearby neurons in cortex has been shown experimentally to sometimes exceed 40 percent (Ko 2011; Levy 2012) suggesting a *small-world* organization of the brain.

The canonical small-world network in the context of neuroscience is one in which the majority of connections in a neural network form small densely connected clusters with respect to the size of larger brain regions. The remaining connections then maintain intermediate communication channels between these islands of dense synaptic connectivity. The conjunction of local clustering and global interaction is thought to provide a structural substrate for the coexistence of functional segregation and integration in the brain (Sporns 2006). However, accessing brain regions in which computations are carried out in a non-perturbative fashion is a long-lasting challenge. In addition, the extremely high dimensional parameter spaces of even small networks of neurons makes a systems-scale understanding of neural computation difficult. However, in an era of high-performance computing there is some hope of contributing to our understanding of functional brain states via *analysis by synthesis*. In the following paragraphs, the progression towards the state of the art for theoretical and

computational models of brain-like neural networks will be summarized.

### 1.2.1 *The diffusion approximation*

Recent experimental advances permit the recording of spike trains of many neurons simultaneously *in-vivo*. These experiments have revealed that significant spatial and temporal correlations exist in the timing of spikes by individual neurons, bringing the role of correlations in neural computation into question. Often, such studies are necessarily contextual - correlations must be interpreted in the context of known stimulus drive, learning or experience, or changes in behavioral context (Cohen 2011). Interpretation of such correlations has been a fruitful exercise; however, it is also important to understand the functional properties of neuronal networks that give rise to them such as topological parameters, stimulus statistics, and synaptic plasticity. For pairs of neurons, correlations are often quantified according to the cross-correlation function of their spike trains (Ostojic 2009). The profile of this cross-correlation function is dependent on several factors including direct synaptic wiring (Snider et al., 1998; Csicsvari et al., 1998; Barthó et al., 2004; Fujisawa et al., 2008) or common and potentially correlated inputs (Sears and Stagg, 1976; Binder and Powers, 2001; Constantinidis et al., 2001; Türker and Powers, 2001, 2002). Although cross-correlation analysis can provide substantial information regarding the topology of a neural circuit, relating the correlations of spike trains to the underlying circuit architecture is a long-lasting problem in computational neuroscience. To approach this problem, simulations of integrate and fire neurons are often used. In these simulations, network parameters are tuned to examine the resulting correlation structure of spike trains with the hope of inverting the model for comparison with *in-vivo* recordings.

In addition to non-trivial correlations in their spike timing, neurons in cortical networks tend to exhibit highly irregular time intervals between spikes. The stochasticity in spike timing has can be attributed to cellular and sensory noise (Faisal 2008), or alternatively

to network-scale mechanisms such as excitatory-inhibitory balance (Vreeswijk 1996, 1998). Amidst this irregularity, our understanding of spike correlations are further complicated by the nonlinear dynamics of recurrent network models (Baker 2019; Tetzlaff 2008, 2012; Doiron 2016; Ocker 2017). It is common to tame this complexity by making suitable combinations of assumptions regarding the statistics of network stimuli, the mechanism of neuron-neuron interactions, or the statistics of synaptic connectivity. In the so-called diffusion approximation, all of these assumptions are involved in order predict features network dynamics, making it a natural starting point for review.

As a rule, the postsynaptic current to a neuron embedded in a spiking network consists of two components: feedforward (sometimes called background) and feedback (sometimes called recurrent):

$$I(t) = F(t) + R(t) \tag{1.1}$$

A variety of models for the integration of this current into a stateful membrane potential exist. For example, the integrate and fire model

$$\tau \dot{V}(t) = \psi(V) + I(t) \tag{1.2}$$

where the function  $\psi(V)$  is an arbitrary function of the membrane potential. To produce spiking behavior, the membrane potential is passed through a special type of activation function or thresholding function which produces neural spike trains

$$z_j(t) = \sum_i \delta(t - t_i) \tag{1.3}$$

where  $t_i$  is the time at which the  $i$ -th spike of neuron  $j$  occurred. A primary goal of modern computational neuroscience is to understand the origins of correlations or lack thereof in the

variable  $z(t)$  across a population of neurons. A first step in this direction is to reveal general principles of the relationship between spike correlations and the interaction between stimulus statistics and the statistics of synaptic connectivity.

Perhaps the most fundamental approximation of the dynamics excitatory-inhibitory networks is the so-called *diffusion approximation* where synaptic currents are assumed to be uncorrelated Gaussian white noise. This approximation is valid in multiple regimes. For example, when synaptic connectivity is sufficiently weak and/or sparse, synaptic inputs to a neuron can be guaranteed to follow a normal distribution, per the central limit theorem. However, the diffusion approximation is not exclusive to these network architectures. It is also a valid assumption when there exists an appropriate cancellation of correlations between feedforward  $F(t)$  and feedback  $R(t)$  synaptic currents, even in dense networks (Rosenbaum 2017). In the following paragraphs the mathematics of the diffusion approximation will be summarized.

In the case that synaptic currents are uncorrelated across an excitatory-inhibitory network, a high dimensional stochastic version of (1.2) describing network dynamics can be collapsed to one dimension. The problem becomes the determination of the membrane potential density over the population as a function of time  $P(V, t)$ . Generally, this can be done by making use of the diffusion approximation of the Kramers-Moyal expansion, also known as the Fokker-Planck equation (Brunel 2000; Brunel and Hakim 1999)

$$\frac{\partial P_j(V, t)}{\partial t} = \frac{\partial}{\partial V_j} [(V_j(t) - \mu_j(t)) P_j(V_j, t)] + \frac{\sigma_j^2(t)}{2} \frac{\partial^2}{\partial V_j^2} [P(V_j, t)] \quad (1.4)$$

Interestingly, the stationary solution of the density  $P(V, t)$  can be found analytically, providing an estimate of steady state firing rates. As expected, uncorrelated synaptic currents produce uncorrelated spike trains, although transitions towards synchrony in this regime have been discussed (Brunel 2000).

As mentioned, additional theoretical work has proposed that the irregular inter-spike intervals observed in cortex can be explained by approximate balance of excitatory and inhibitory synaptic currents (Vreeswijk, 1996). In this balanced regime, the timing of the firing of cells in cortex is sensitive to the relatively small fluctuations in their total synaptic input because the excitatory and inhibitory inputs cancel each other (Amit, 1995). Also, excitatory and inhibitory balance has been theoretically shown to enhance the sensitivity of fast stimulus fluctuations much smaller than a typical integration time constant for a single neuron (Vreeswijk, 1996; Tian 2020). Interestingly, model neurons optimally detect temporal information when the average membrane potential is one standard deviation of the noise below threshold, a phenomenon known as stochastic resonance (Plesser, 2000; Kempter, 1998). Importantly, a general framework for generating balanced networks has been developed. In the following paragraphs, the terminology and mathematical machinery introduced in (Vreeswijk 1996) and later used by (Renart 2010; Rosenbaum 2017) will be described.

A network model is called *sparse* if the probability of a connection between a neuron in a population  $\alpha$  and another neurons in a population  $\beta$  scales with the network size  $N$  according to  $p_{\alpha\beta} \sim \mathcal{O}(1/N)$ . Using terminology borrowed from graph theory, the degree  $K$  of a neuron does not depend on the scale of the network or  $K \sim \mathcal{O}(1)$ . In contrast, we then say that a network is *dense* if the above connection probability scales as  $p_{\alpha\beta} \sim \mathcal{O}(1)$  such that the degree of a neuron scales as  $K \sim \mathcal{O}(N)$ . Moreover, the efficacy of a synaptic connection between populations  $\alpha$  and  $\beta$  is said to be *strong* if  $J_{\alpha\beta} \sim \mathcal{O}(1)$  and *weak* coupling occurs when  $J_{\alpha\beta} \sim \mathcal{O}(1/\sqrt{N})$ . This choice of scaling for  $J_{\alpha\beta}$  and the degree  $K$  results in the total synaptic input to a neuron scaling as  $\mathcal{O}(\sqrt{N})$ . In this case, it is possible parameterize the network s.t. fluctuations in the synaptic input currents saturates to a value of the order of the spiking threshold, in the limit of large  $N$  (Vreeswijk, 1996; Renart 2010; Rosenbaum 2017).

The scaling of synaptic inputs outline above are a critical step towards finding the balanced state. To see this, consider the total synaptic current injected into a neuron  $i$  within a population  $\alpha$ , decomposed into its feedforward and recurrent components

$$I_i^\alpha(t) = F_i^\alpha(t) + R_i^\alpha(t) \quad (1.5)$$

$$= F_i^\alpha(t) + \sum_{\beta} \sum_j \frac{J_{ij}^{\alpha\beta}}{\sqrt{N}} (\psi * z_j^\beta(t)) \quad (1.6)$$

where the variable  $z_j^\beta(t)$  is sometimes called the *observable state* of neuron  $j$  and is given by thresholding the voltage:  $z_j^\beta(t) = H(v_j^\beta(t) - \theta)$  where  $H$  is the Heaviside step function. For the sake of generality, the term  $z_j^\beta(t)$  is convolved with a kernel  $\psi$ , determining the shape of the post-synaptic potential induced by a spike. In the mean-field approximation we replace the current in each term of the sum over  $j$  in (1.2) by its average value, which is a valid approximation in the limit  $N \rightarrow \infty$  (Vreeswijk 1996). Taking  $\psi = \delta(t)$ , the observable state  $z_j^\beta(t)$  is replaced by the average firing rate of a neuron in population  $\beta$  multiplied by the probability of a connection  $p_{\alpha\beta}$

$$\begin{aligned} \langle I_i^\alpha(t) \rangle &= \langle F_i^\alpha(t) \rangle + \langle R_i^\alpha(t) \rangle \\ &= \langle F_i^\alpha(t) \rangle + \sqrt{N} \sum_{\beta} j_{\alpha\beta} p_{\alpha\beta} r_{\beta} \end{aligned}$$

with  $j_{\alpha\beta} = J_{\alpha\beta} \sqrt{N}$ . Notice that the average value of the recurrent contribution to the synaptic current indeed saturates for large  $N$ . Writing the above equation explicitly for a neuron in an excitatory-inhibitory network i.e.  $\alpha, \beta \in \{e, i\}$



$$\langle I_j^e(t) \rangle = \langle F_j^e(t) \rangle + \sqrt{N} (j_{ee} p_{ee} r_e + j_{ie} p_{ie} r_i) \quad (1.7)$$

$$\langle I_k^i(t) \rangle = \langle F_k^i(t) \rangle + \sqrt{N} (j_{ii} p_{ii} r_i + j_{ei} p_{ei} r_e) \quad (1.8)$$

If we require that, in the mean-field limit  $N \rightarrow \infty$ , the average current vanishes and that  $\langle F_j^\alpha(t) \rangle \sim \mathcal{O}(\sqrt{N})$  we have the following matrix equation relating the mean field firing rates to the synaptic weights and average feedforward current

$$\begin{pmatrix} j_{ee} & j_{ie} \\ j_{ei} & j_{ii} \end{pmatrix} \begin{pmatrix} r_e \\ r_i \end{pmatrix} = - \begin{pmatrix} \langle F_j^e \rangle \\ \langle F_k^i \rangle \end{pmatrix} \quad (1.9)$$

which can be summarized as  $\mathbf{r} = -\mathbf{J}^{-1}\mathbf{f}$ . Assuming that  $\mathbf{J}$  is invertible, we have the following solution

$$\lim_{N \rightarrow \infty} r_e = \frac{\langle F_j^e \rangle j_{ii} - \langle F_k^i \rangle j_{ie}}{j_{ei} j_{ie} - j_{ee} j_{ii}} \quad (1.10)$$

$$\lim_{N \rightarrow \infty} r_i = \frac{\langle F_k^i \rangle j_{ee} - \langle F_j^e \rangle j_{ei}}{j_{ei} j_{ie} - j_{ee} j_{ii}} \quad (1.11)$$

For positive solutions for the above firing rates and for the above matrix to be invertible we have the rather loose condition  $\langle F_j^e \rangle / \langle F_k^i \rangle > j_{ie} / j_{ii} > j_{ee} / j_{ei}$  and we recover the condition given in (Rosenbaum 2014; Rosenbaum 2017; Akil 2021).

**Make a stronger argument for why the inputs are uncorrelated in the asynchronous state**

Since the balanced state is simultaneously an asynchronous state, the recurrent inputs  $R_i$

are uncorrelated and can be written as a gaussian random variable

$$R_i(t) = \sqrt{N}\mu_R(t) + \sigma_R(t)\xi_R(t)$$

where  $\mu_R^\alpha = (j_{e\alpha}p_{e\alpha}r_{e\alpha} + j_{i\alpha}p_{i\alpha}r_{e\alpha})$  and  $\sigma_R^\alpha = (j_{e\alpha}^2p_{e\alpha}r_{e\alpha} + j_{i\alpha}^2p_{i\alpha}r_{e\alpha})$  (Brunel 2000).

Assuming the feedforward current  $F_i(t)$  is also uncorrelated, the total current is also a gaussian random variable

$$I_i(t) = \sqrt{N}\mu_I(t) + \sigma_I(t)\xi_R(t)$$

using the shorthand  $\mu_I(t) = \mu_F(t) + \mu_R(t)$  and  $\sigma_I(t) = \sigma_F(t) + \sigma_R(t)$ . The Fokker-Planck equation in (1.5) then applies, and in the steady-state becomes

$$\frac{\sigma_I^2(t)}{2} \frac{\partial^2}{\partial V^2} [P(V, t)] = \frac{\partial}{\partial V} [(V(t) - \mu_I(t)) P(V, t)] \quad (1.12)$$

Due to the firing threshold  $\theta$ , boundary conditions on the above equation must be imposed (Brunel and Hakim 1999; Brunel 2000)

$$\begin{aligned} P(V, t) &= 0, v \geq \theta \\ P(v_r^-, t) &= P(v_r^+) \\ \frac{\partial P(v_r^+, t)}{\partial t} - \frac{\partial P(v_r^-, t)}{\partial t} &= \frac{\partial P(\theta, t)}{\partial t} \\ \int_{-\infty}^{\theta} P(V, t) dV &= 1 \end{aligned}$$

### 1.2.2 *Beyond the diffusion approximation*

More recently, neuroscientists have developed a framework for understanding spike train correlations beyond the diffusion approximation. This development has been motivated by the fact that the integration of temporally correlated presynaptic spike trains can result in non-trivial two-point correlation functions that are not well-described by a Gaussian white noise process (Moreno-Bote 2008). In addition, recent experiments have shown that local cortical networks can be dense with connection probabilities sometimes exceeding 40 percent (Ko 2011; Levy 2012; Fino 2011). A novel approach, based on linear response theory, lifts the diffusion approximation and makes predictions on spike correlations directly in terms of circuit architecture (Ocker 2017). More specifically, by making use of a linear response theory, one can derive the matrix of auto and cross-spectra of spike trains in terms of synaptic coupling matrices directly (Pernice 2011; Trousdale 2013; Ocker 2017).

In essence, a linear response theory of network dynamics determines the auto and cross spectra of spike trains by assuming a linear relationship between the output firing rate of a neuron and its presynaptic input spikes. For example, the approach pioneered by Pernice et al. leverages Hawkes theory of linearly interacting point processes to calculate stationary firing rates and spike correlations in excitatory-inhibitory networks (Pernice 2011, 2012). Put simply, if neural spike trains are taken to be realizations of heterogeneous Poisson processes i.e.  $r_i(t) = \langle z_i(t) \rangle$ , Hawkes theory can be used to estimate the vector of firing rates  $\mathbf{r}(t)$ . To do this, we first define a matrix  $G(\tau)$  which can be convolved with the vector of spikes  $\mathbf{z}(\tau)$  to give the linear influence of  $\mathbf{z}(\tau)$  on the firing rates  $\mathbf{r}(t)$ . The matrix element  $g_{ij}(\tau)$  represents the linear influence of a spike of neuron  $i$  on the firing rate of neuron  $j$  which can be computed as the normalized covariance of a Poisson spike train  $z_i$  with  $z_j$  (Pernice 2012)

$$g_{ij}(J_{ij}, \tau) = J_{ij}a_{ij}(\tau) \tag{1.13}$$

where we have the following expression for the interaction kernel  $a_{ij}(\tau)$  in the time-domain

$$a_{ij}(\tau) = \frac{\langle z_i(t+\tau), z_j(t) \rangle - \langle z_i(t+\tau) \rangle \langle z_j(t) \rangle}{\langle z_i(t) \rangle} \quad (1.14)$$

which is the normalized cross-covariance of point processes (spike trains)  $z_i$  and  $z_j$ . Packaging  $g_{ij}(J_{ij}, \tau) \quad \forall i, j$  into a matrix  $G(\tau)$ , the vector of firing rates is predicted by the convolution of  $G(\tau)$  and  $z(\tau)$  in the time-domain

$$r(t) = r_0 + \int_{-\infty}^{\infty} G(t-\tau) z(\tau) d\tau \quad (1.15)$$

We then have the following steady-state matrix of cross-covariances in the time domain (Pernice 2012; Ocker 2017)

$$C_0(\tau) = G(\tau) R_0 + (G * C_0)(\tau) \quad (1.16)$$

Noting that the Fourier transform of a Poisson process with rate  $r_i$  takes the value  $r_i$  for all frequencies in the frequency domain, we can find the cross spectral matrix  $C(\omega)$  as (Pernice 2012)

$$C(\omega) = [1 - G(\omega)]^{-1} R_0(\omega)(\omega) [1 - G^*(\omega)]^{-1} \quad (1.17)$$

$$= \Delta(\omega) R_0 \Delta^*(\omega) \quad (1.18)$$

where the Fourier transform of the rates has been arranged as a diagonal matrix. Recently, the matrix  $\Delta(\omega)$  has been termed a *propagator* as it propagates the rates of each neuron to the rest of the population (Ocker 2016). Also,  $\Delta(\omega) = (I - A(\omega)J)^{-1}$ , taking the fourier

transform of the interaction kernel in (1.14) and organizing this as a diagonal matrix  $A(\omega)$ . Furthermore, the solution for  $C(\omega)$  has been extended to also account for correlations in feedforward inputs (Ocker 2015; Ocker 2016)

$$C(\omega) = \Delta(\omega) R_0 \Delta^*(\omega) + \Delta(\omega) A(\omega) C^{\text{ext}}(\omega) A^*(\omega) \Delta^*(\omega) \quad (1.19)$$

After taking the inverse Fourier transform, we then have the cross-covariance matrix where correlations can arise from both feedforward and recurrent activity. In summary, the linear theory provides a direct mechanism for solving for the cross-covariance of spiking in the population in terms of the synaptic coupling matrix, for arbitrary network topologies. Previous analyses have restricted feedforward inputs to be uncorrelated and have considered only random networks (Pernice 2012). Other analyses have considered more complex networks, such as Erdos-Renyni networks with a spike-timing dependent plasticity rule, but have left external input uncorrelated (Ocker 2015).

### 1.2.3 *Reshaping network structure with synaptic plasticity*

Activity dependent modification of synaptic efficacy or the formation of new synapses is the putative basis of learning and memory formation. In his famous neurophysiological postulate, Donald Hebb suggested that repeated stimulation of specific receptors of sensory signals would lead to the formation of a *cell assembly* and these structural changes would constitute a representation or imprint of an internally or externally generated sensation (Hebb 1949). The chaining of these assemblies then could provide a structural basis for cognitive processes such as memory retrieval, reasoning, and planning (Buzaki 2010). Recent neurobiological advances have provided substantial insight on the biochemical and biophysical mechanisms of plasticity. However, the formation of functional circuits and their stability amidst ongoing

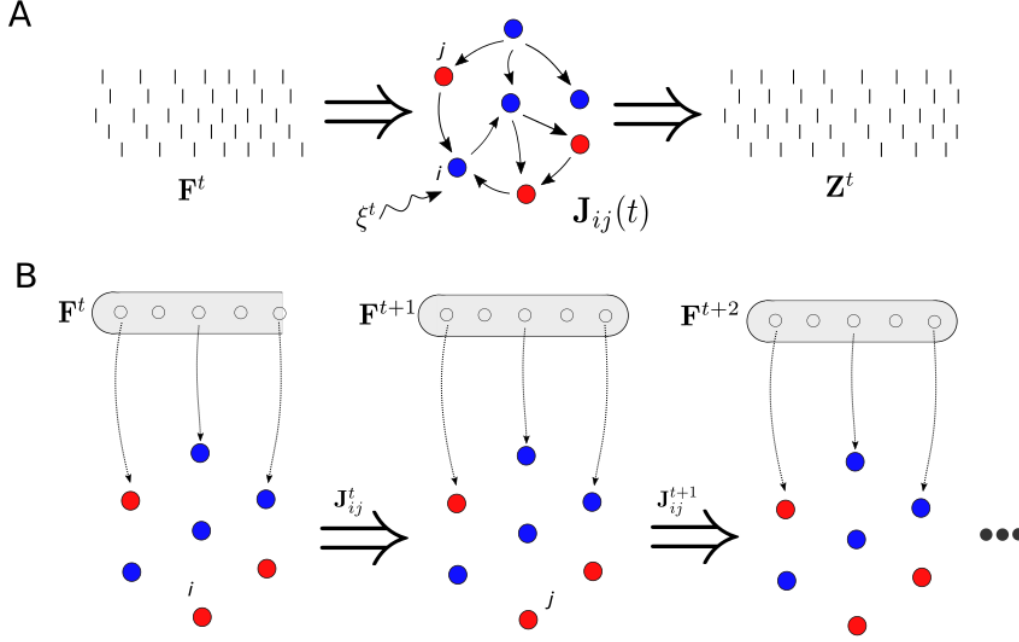


**Figure 1.1:** (a) Diagram of a recurrent neural network receiving a time-dependent feed-forward stimulus. (b) Diagram of the stochastic encoding scheme used a recurrent neural network with noise

network dynamics remains unclear.

Plasticity mechanisms are highly diverse and occur over a wide range of time scales: from milliseconds to hours to days (Zenke 2015). For example, short-term synaptic plasticity (STP) is thought to provide a richer set of network responses to stimuli without permanently altering the circuit architecture. One of several mechanisms thought to underly STP can be seen by the repeated stimulation of a presynaptic cell causing a transient accumulation of calcium in the presynaptic terminal, which has been proposed as a mechanism for short-term memory (Mongillo 2008). Calcium ions elevate the probability of neurotransmitter release due to its proposed interaction with the biochemical machinery involved in synaptic vesicle exocytosis. Other short term changes in synaptic efficacy can occur such as the facilitation or depression based upon the temporal characteristics of the stimulus. Paired-pulse experiments have yielded evidence that tetanic stimulation can result in inactivation of voltage-dependent

sodium and/or calcium channels or depletion of the release ready pool of synaptic vesicles at the presynaptic terminal. Synaptic efficacy can alternatively be lowered by the release of biochemical neuromodulators which can interact with the synaptic machinery to inhibit the release of neurotransmitter into the synaptic cleft. Thus, these neuromodulators can also play a role in facilitation or depression in STP.

It is well-accepted that neural circuits also possess the mechanisms for long term changes in synaptic strength formally referred to as long term potentiation (LTP) and long term depression (LTD). The brain encodes internally and externally generated stimuli as spatiotemporal patterns of action potentials and long-term modifications to such patterns via changes in synaptic transmission provide a feasible mechanism for the storage of information. In other words, permanent or semi-permanent changes in synaptic weights alter the spatiotemporal response of population of neurons to stimuli and therefore provide a method for long term memory formation. Since its inception by Cajal, this idea has been rigorously tested, for example in the CA1 region of the hippocampus (Whitlock et al. 2006). The modification of spatiotemporal characteristics of the neural response to stimuli suggest that evidence for plasticity can be found in the correlation structure of neural spike trains.

Early work on synaptic plasticity at the cellular level demonstrated that LTP in slices of hippocampal tissue could occur as a result of tetanic (high-frequency) stimulation of a postsynaptic cell (Bliss 1973) while low frequency stimulation can drive LTD. If many fibers are stimulated at frequencies exceeding 50Hz, postsynaptic potentials can increase by 50-100% (Sejnowski 1989). Additional research expanded upon this observation, noting that temporal correlation of presynaptic and postsynaptic spiking affected plasticity. In particular, strong temporal correlation on a timescale of  $\pm 100\text{ms}$  gave rise to LTP while weak correlations LTD. These phenomenological studies of plasticity have resulted in a number of different plasticity rules which fall under the umbrella of ‘Hebbian’ learning rules. Hebbian learning rules have been broadly defined as rules in which the change in synaptic efficacy depends only on pre-

synaptic and post-synaptic variables and that updates to the weight depends interactively on these two variables and not separately (Sejnowski 1989). Additionally, Hebbian learning rules are *causal* in that LTP occurs when the presynaptic neuron contributes to the firing of the postsynaptic cell and LTD occurs otherwise.

Additional efforts demonstrated that the sign and magnitude of LTP and LTD depend on the order and delay of presynaptic and postsynaptic action potentials, on a time scale of 10ms (Markram 1997), later named spike timing dependent plasticity (STDP) (Song 2000). In the original formulation of Hebbian STDP, LTP can occur when presynaptic spikes lead postsynaptic spikes by  $\sim 20$ ms and LTD can occur when postsynaptic spikes lead presynaptic spikes by  $\sim 20 - 100$ ms (Markram 1997; Bi and Poo 1998; Celikel 2004; Feldman 2012). However, plasticity does not only depend on spike timing, but also on other factors such as firing rates, and synaptic cooperativity, and postsynaptic voltage (Markram 1997; Sjostrom 2001; Feldman 2012). Therefore, findings indicate that STDP is part of a broader class of plasticity rules and may be viewed as the spike timing component of a multifactor plasticity rule (Feldman 2012).

Furthermore, the biochemical mechanism of synaptic plasticity is regulated by the release of neurotransmitters by the presynaptic cell and/or by modifying the density of receptors at the postsynaptic membrane (Sumi 2020). Indeed, it is widely believed that presynaptic release of glutamate results in activation of  $\alpha$ -amino-3-hydroxy-5-methyl-4-isoxazolepropionic acid receptor (AMPA) and subsequent depolarization of the post-synaptic membrane. Membrane depolarization then activates the N-methyl-D-aspartate receptor (NMDAR), which is permeable to  $\text{Ca}^{2+}$  - a precursor for a biochemical cascade resulting partially in the trafficking of AMPA receptors to the postsynaptic membrane. High elevations in  $\text{Ca}^{2+}$  concentrations in the presynaptic cell are believed to result in an increased density of AMPA receptors at the postsynaptic membrane and in elevated excitatory postsynaptic potentials (EPSPs) thereby providing a mechanism for LTP (Sumi 2020). In summary, LTP versus LTD induction is



determined by the magnitude and time course of calcium flux (Lisman 1989; Yang 1999; Feldman 2012). When the presynaptic cell fires first, the EPSP produces a strong NMDAR calcium flux while while when the postsynaptic cell fires first, this flux is weak. On the other hand, LTD has not been shown to occur solely due to minor elevations in  $\text{Ca}^{2+}$  concentrations, but is thought to result from a retrograde signaling mechanism in which presynaptic transmitter release probability is decreased (Nabavi 2013).

Beyond spike-timing dependent plasticity, other plasticity mechanisms have been observed experimentally. In the hippocampus, non-Hebbian heterosynaptic LTD alongside LTP was described shortly after the phenomenon of LTP was discovered (Lynch 1977). The Hebbian mechanisms or *associative mechanisms* discussed above are termed homosynaptic mechanisms, as they depend on both pre- and post-synaptic activity. There are also heterosynaptic mechanisms which depend on only the state of the post-synaptic neuron and are thought to exist to counteract chaotic dynamics introduced by Hebbian-type rules and to balance synaptic changes (Chistakova 2014). Hebbian homosynaptic learning rules, by definition, potentiate (depress) synapses with positive feedback, meaning that increasing (decreasing) synaptic efficacy will promote further potentiation (depression). For example, The standard doublet STDP model gives rise to splitting of synaptic weights, producing a bimodal distribution; however, weight distributions observed in experiments are unimodal and long-tailed (Perin 1997; Song 2005). The result is the overexcitability of some neurons and silencing of others making network dynamics unstable. Induction of LTD at high firing rates of the postsynaptic neuron is a candidate for an intrinsic stabilization mechanism (Kempster 2001). Also, it has been recently suggested that rate-dependent terms in the synaptic learning rule can stabilize motif configurations (Ocker 2015). Ultimately, it is thought that a push-pull mechanism exists in which homosynaptic LTP prevents the network from falling silent at low firing rates while heterosynaptic LTD prevents the runaway dynamics at high firing rates.

Understanding the stable formation and maintenance of cell assemblies is an additional goal of synaptic plasticity research. From a naive point of view, a cell assembly could form if a subset of a neuron’s inputs were to potentiate while other inputs depress. However, for this to occur both groups should be repeatedly activated either with highly specific patterns to promote LTP or LTD, respectively (Chistikova 2014). This would then limit network stability to special sequences of input patterns while we expect that plasticity mechanisms exist to promote stability under a variety of input stimuli. Moreover, experiments involving intercalated neurons of the amygdala have demonstrated that LTP induction with high-frequency stimulation can simultaneously result in heterosynaptic depression (Royan 2003). Conversely, LTD induction with low-frequency stimulation was also shown to induce LTP. These observations indicate the existence of intracellular signaling that would provide synapses with ‘awareness’ of each other. Learning rules which depend on the post-synaptic firing rate would produce a similar result, although often these rules do not perform selective potentiation or depression. That is, synaptic weights are normalized without regard to which synapses can be blamed for chaotic or silent neuron states. In circuits with highly regular organization of the inputs, such as the hippocampus or amygdala, the onset of LTP can induce weaker LTP at nearby inputs while concurrently inducing heterosynaptic LTD at more distant inputs, while the magnitude of LTD decreases with distance (Royer 2003; White 1990).

The experimental observations discussed suggest that balanced LTP and LTD may be a powerful mechanism for synaptic normalization and synaptic competition. Thus, several computational studies incorporating more realistic forms of synaptic plasticity with conductance based neuron models have surfaced e.g., (Zenke 2015; Kumar 2014). Many have incorporated a balance between excitation and inhibition to capture the irregular activity of cortical networks, but stable formation of cell assemblies is difficult to achieve. This shortcoming could, in part, be due to the tendency of STDP to lead to pathological behavior in balanced networks (Morrison 2007). The introduction of homeostatic mechanisms such as

normalization of total excitatory conductance alongside inhibitory STDP to control the firing rate of excitatory neurons has been used to inhibit pathological activity in the balanced regime (Kumar 2014). At the same time, the spatial properties of homeostatic plasticity mechanisms mentioned above have yet to be investigated. This, in combination with spatially dependent connection probabilities as in (Rosenbaum 2017) could provide insight into the stability of cell assemblies.

In plastic networks, synaptic weights (conductances) are functions of time, thus we expand  $I(t)$  as a sum of individual conductances as in (Zenke 2015) to give a total current for a single neuron

$$\begin{aligned} I_j^\alpha(t) &= \sum_{\beta} \sum_i g_{ij}^\beta(t) (E_\beta - V_j) \\ &= \sum_{\beta} \sum_i J_{ij}^{\alpha\beta}(t) (\phi * z_i(t)) (E_\beta - V_j) \end{aligned}$$

where  $\alpha \in \{E, I, X\}$ . To be clear, excitatory conductances, whether in the external or primary population would be under the control of an inhibitory neurotransmitter such as gamma-aminobutyric acid (GABA) while inhibitory conductances would be under the control of glutamate e.g., AMPAR/NMDAR. Notice that the time-dependence of  $g^\alpha$  can then be given by the convolution of an excitatory presynaptic spike train  $z_i(t)$  or inhibitory spike train  $z_k(t)$  with an appropriate synaptic kernel  $\phi$ . The synaptic plasticity rule is then a rule for the time-derivative  $j_{ij}^{\alpha\beta}$ .

The cellular machinery of plasticity mechanisms described above highlights the importance of spike-time correlations, generated by recurrent feedback or feedforward projections, in determining the evolution of synaptic weights. A classic derivation of the evolution of synaptic weights for interacting Poisson processes was given by Kempter et al. (Kempter 1999). This result is an important starting point for later analysis. Consider the total change

in the synaptic weight between neurons  $i$  and  $j$  as  $\Delta J_{ij} = J_{ij}(t + \Delta t) - J_{ij}(t)$  in a time interval  $\Delta t$ . Consider the very general rule for a single spiking neuron  $i$  receiving many inputs  $1 < j \leq N$

$$\dot{J}_{ij} = a_0 + a_i z_i(t) + a_j z_j(t) + F(z_i(t), z_j(t))$$

for a yet unknown function  $F$ , which could be a STDP rule, for example. We will assume that the constant growth or decay term  $a_0$  is zero. Spike trains are a summation of delta functions over time, i.e.  $z_i(t) = \sum_n \delta(t - t_i^n)$  and  $z_j(t) = \sum_m \delta(t - t_j^m)$ . If we consider only rules that consider the timing of pairs of spikes, changes in synaptic weight can occur from the arrival of a presynaptic spike  $z_i(t) = 1$ , a postsynaptic spike  $z_j(t) = 1$  or as a function of the delay in spike timing  $\tau = t_i^n - t_j^m$ . The spike-timing component of the learning rule is given by the learning window function  $W(t_i^n - t_j^m)$ . Integrating over a time window  $\Delta T_{\text{lrn}}$  gives the total change  $\Delta J_{ij}$  (Kempster 1999)

$$\Delta J_{ij}(\Delta T_{\text{lrn}}) = \int_0^{\Delta T_{\text{lrn}}} dt' (a_i z_i(t') + a_j z_j(t')) \quad (1.20)$$

$$+ \int_0^{\Delta T_{\text{lrn}}} dt' \int_0^{\Delta T_{\text{lrn}}} dt'' W(\tau) z_i(t'') z_j(t') \quad (1.21)$$

The stochasticity of the spike functions  $z_i(t)$  and  $z_j(t)$  means that we can only hope to derive the behavior of the above integral on average. In other words,  $\Delta J_{ij}$  is itself a stochastic process but we can focus on its drift or expected rate of change. Simultaneously,  $z_i(t)$  and  $z_j(t)$  are strongly dependent on the weights  $J_{ij}$ ; however, if the time scale of plasticity  $\Delta T_{\text{lrn}}$  is sufficiently long compared to the correlation time scale of the neurons activity, the correlation between  $z_i(t)$  and  $z_j(t)$  can be treated as stationary (Kempster 2001). Importantly, the effective correlation time scale of neuron dynamics is intimately related to the timescale over which it is ‘picked up’ by the learning window  $W(\tau)$ . Analyzing the drift

in  $\Delta J_{ij}$  then reads

$$\begin{aligned} \Delta T_{\text{lrn}} \frac{\langle \Delta J_{ij} \rangle(t)}{\Delta T_{\text{lrn}}} &= \int_0^{\Delta T_{\text{lrn}}} dt' (a_i z_i(t') + a_j z_j(t')) \\ &+ \int_0^{\Delta T_{\text{lrn}}} dt' \int_{-t'}^{\Delta T_{\text{lrn}} - t'} d\tau W(\tau) \langle z_i(t' + \tau) z_j(t') \rangle \end{aligned}$$

Note that we can make the same approximations for a sufficiently slow process as we can for a relatively fast process with high time resolution. Then, if synaptic plasticity is sufficiently slow, then we can approximate the average rate of change as  $dJ_{ij}/dt \approx \Delta J_{ij}/\Delta T_{\text{lrn}}$ , and the bounds of integration can be set to  $-\infty$  and  $+\infty$  (Kempster 1999) and we have the final result

$$\Delta T_{\text{lrn}} \frac{dJ_{ij}(t)}{dt} = a_i \langle z_i(t) \rangle + a_j \langle z_j(t) \rangle + \int_{-\infty}^{+\infty} d\tau W(\tau) C_{ij}(\tau) \quad (1.22)$$

where  $\langle z_i(t) \rangle$  and  $\langle z_j(t) \rangle$  can be interpreted as the instantaneous firing rate of neurons  $i$  and  $j$ , respectively. It has already been shown that linear response theory can be used to estimate  $C_{ij}(\tau)$  for arbitrary network topologies (Pernice 2012). Furthermore, the equation (1.22) including the instantaneous post-synaptic firing rate can serve as a homeostatic term if  $a_j < 0$ . Although, as highlighted previously, rate-dependent terms in the learning rule do not selectively enforce LTP and LTD since the term  $a_j \langle z_j(t) \rangle$  appears in the equation for  $\dot{J}_{ij}$  for all input neurons  $i$  (assuming  $a_j$  is a constant). Thus we need to modify (1.22) to arrive at a synaptic plasticity rule which delivers potentiation or depression heterogeneously, for example using information regarding spatial proximity. Interestingly, a class of spatially connected networks has been studied (Rosenbaum 2011, 2017).

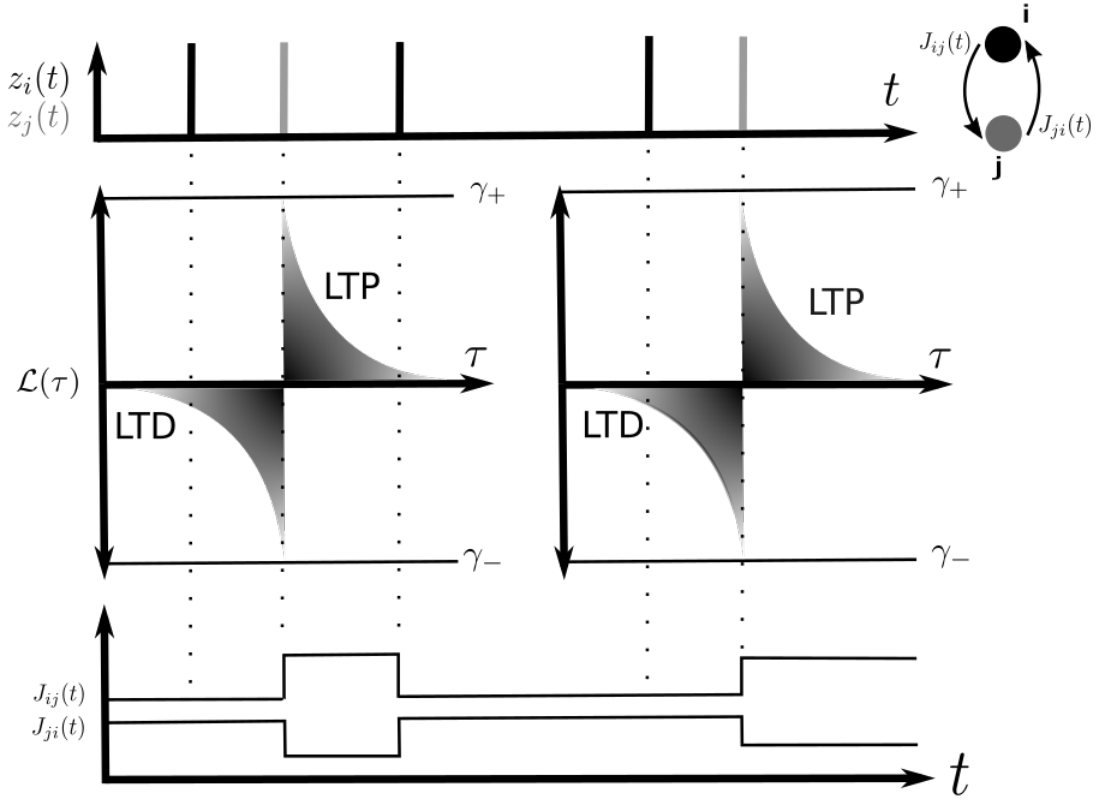


**Figure 1.2:** Computational graph describing the update of synaptic weights  $J_{ij}$  and the cross-covariance matrix  $C(\tau)$  over multiple stimulus blocks of length  $\Delta T_{\text{stim}}$ . The learning period  $\Delta T_{\text{lrn}} \ll T_{\text{stim}}$  determines the frequency of learning updates within the period  $\Delta T_{\text{stim}}$

Say we have the learning window function  $W(\tau)$  corresponding to the standard doublet spike-timing dependent plasticity rule

$$W(\tau) = \begin{cases} H(J_{\max} - J_{ij})\gamma_+ \exp(-\tau/\tau_+), & \text{if } \Delta t \geq 0 \\ H(J_{ij})(-\gamma_-) \exp(-\tau/\tau_-), & \text{if } \Delta t < 0 \end{cases}$$

### 1.2.4 *Reflecting on the interpretation of network dynamics*

Early theoretical models of neural networks frequently made reference to concepts born in the theory of dynamical systems. Sensory processing was often interpreted as an attraction of the neural state variables to a steady state corresponding to the encoding of the sensory stimulus. This point of view adopts the notion that sensory stimuli are then represented in the brain by *attractor states* or locations in phase space which the network is driven towards during sensory processing (Hopfield, 1982). On the other hand, recent experimental evidence suggests that neurons, synapses, and neural systems are inherently stochastic (Buesing 2011). These observations have provoked a dramatic paradigm shift in the way we view computations as being carried out in the brain. Namely, researchers now widely believe that in some cases information processing by the brain can be interpreted as a form of probabilistic inference.

Variability in sensory stimuli and the biological constitution of networks of neurons require the brain to make inferences about the external world amidst uncertainty. For example, the perception of objects in the external world by an organism is, in part, the transformation of a noisy continuously valued variable to a discrete mental representation of the object. The injection of stochasticity into the pathway mapping stimuli to their neural representation has led many to believe that networks of neurons represent probability distributions rather than implementing logical circuits. Interestingly, behavioral studies have confirmed that human observers not only take uncertainty into account in a wide variety of tasks, but do so in a way that is nearly optimal (Ma 2006). It stands to reason that variability in sensory stimuli and performing inference amidst uncertainty are two sides of the same coin. If sensory stimuli were not variable, meaning that the mapping of sensory stimuli to neural responses was deterministic, the neural response from trial to trial would be identical. Therefore, the ability to handle small variations in the stimulus and the ability to generalize would be diminished.

A typical inference scenario is the deduction of the probability that the observed infor-

mation was drawn from a distribution already known by the model. That is, the encoding scheme during sensory processing is the distribution of responses conditioned on the stimulus i.e., the posterior distribution  $P(R|S)$ . In the context of biological and artificial neural networks, that distribution is often *learned* by the model via previous exposure to a large number of samples from the so-called population distribution of the data or stimulus. A popular point of view is that neural activity can be expressed in discrete-time and the set of spikes in each time bin can be interpreted as samples from the posterior  $P(R|S)$ , a distribution which is encoded by the synaptic weights. This interpretation has spawned the development of interesting parallels between neural dynamics and statistical sampling processes such as Markov chain Monte Carlo (MCMC) sampling (Buesing 2011). However, the interpretation of neural dynamics as implementing an artificial sampling process as in the Boltzmann machine, necessarily excludes biological details, such as synaptic plasticity and spike-adaptation, which are thought to play a major role in neural computation.

## 1.3 Results

### 1.3.1 *The two-dimensional Gaussian network*

Suppose that we have a two-dimensional lattice which contains points separated by a distance  $\Delta$  along the axial directions with periodic boundary conditions. The distance between any two points on such a lattice is the following Euclidean distance metric

$$|\Delta \mathbf{r}_{ij}|^2 = \min(|x_1 - x_2|, n\Delta - |x_1 - x_2|)^2 + \min(|y_1 - y_2|, n\Delta - |y_1 - y_2|)^2$$

Now, let the kernel  $\Gamma_{ij}$  be the two-dimensional symmetric Gaussian



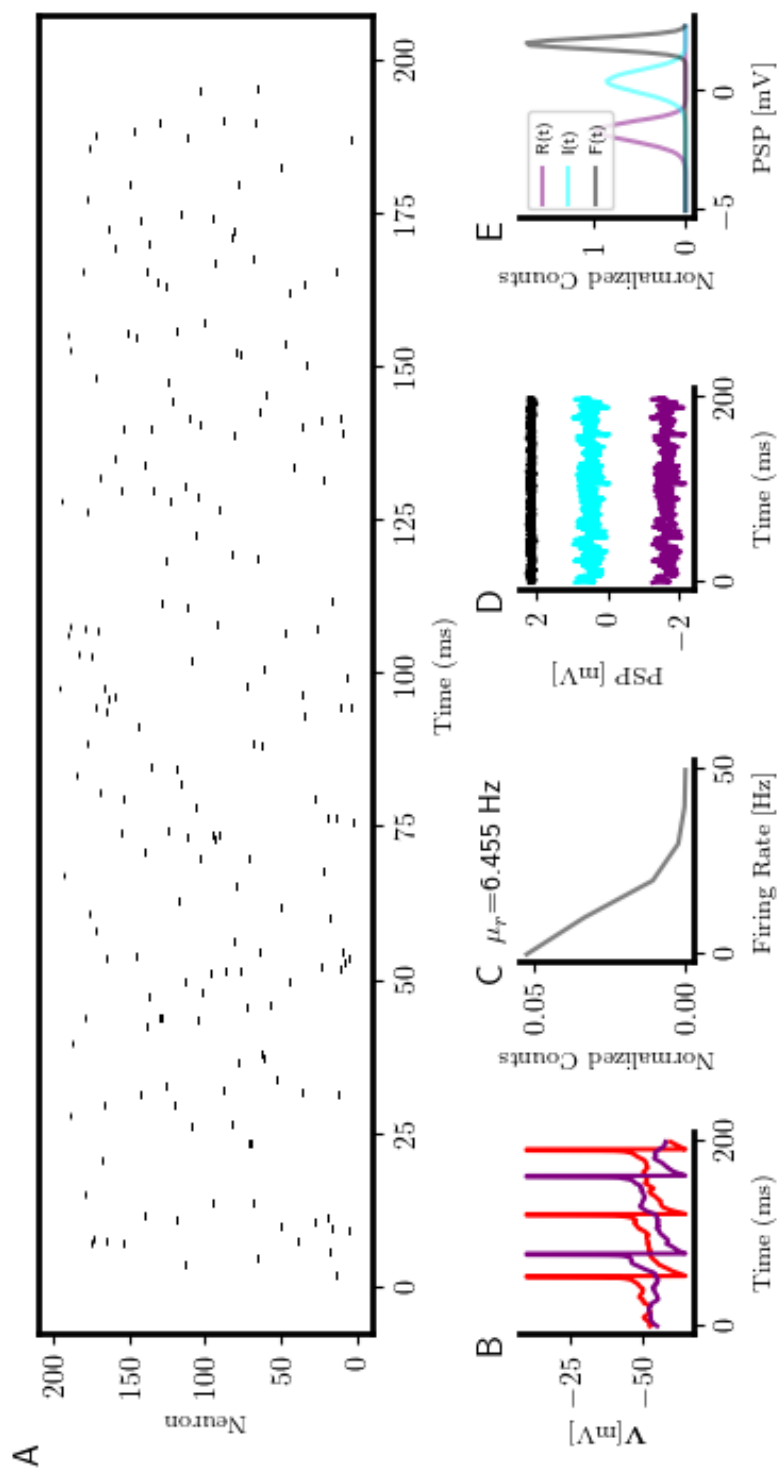


Figure 1.3

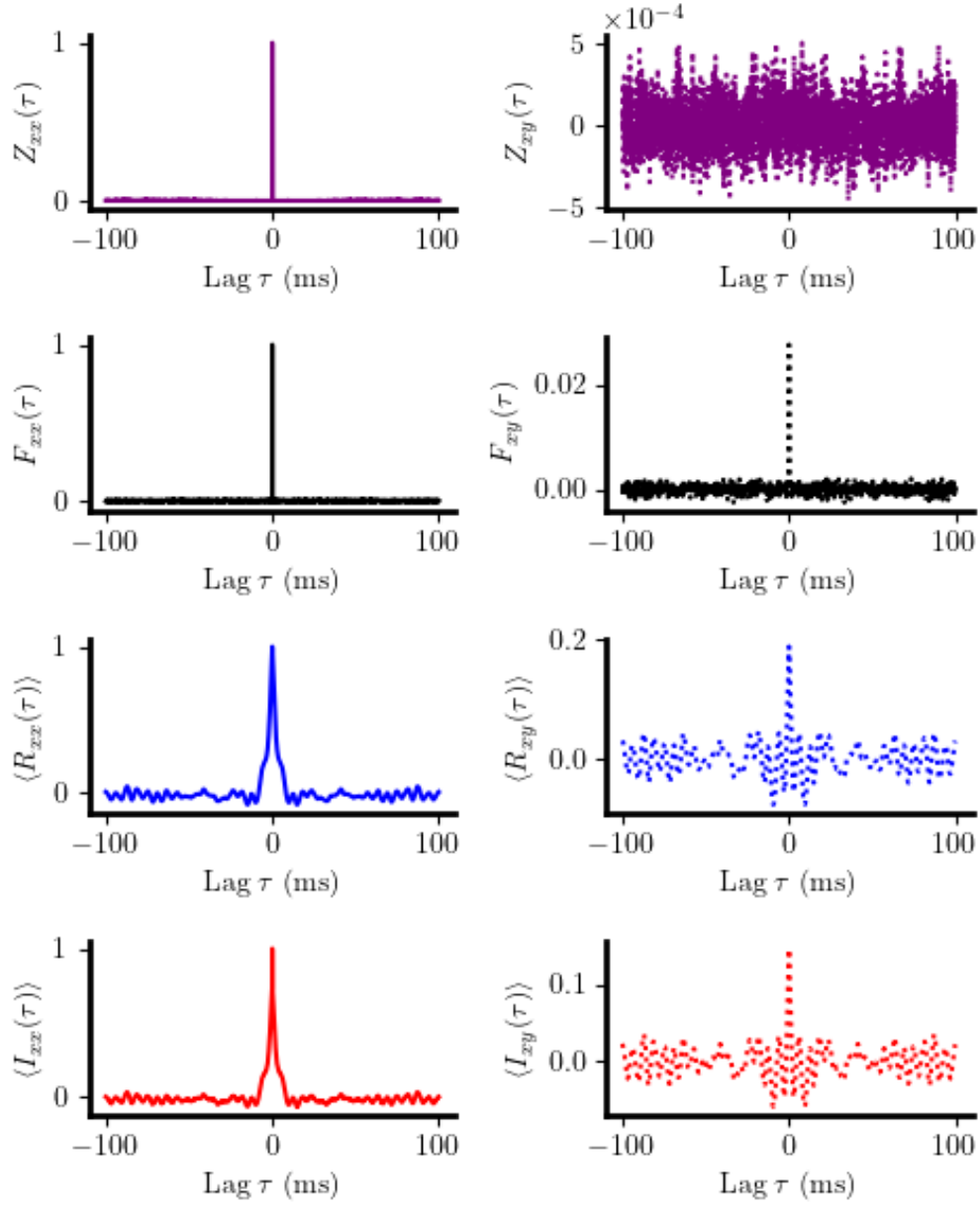
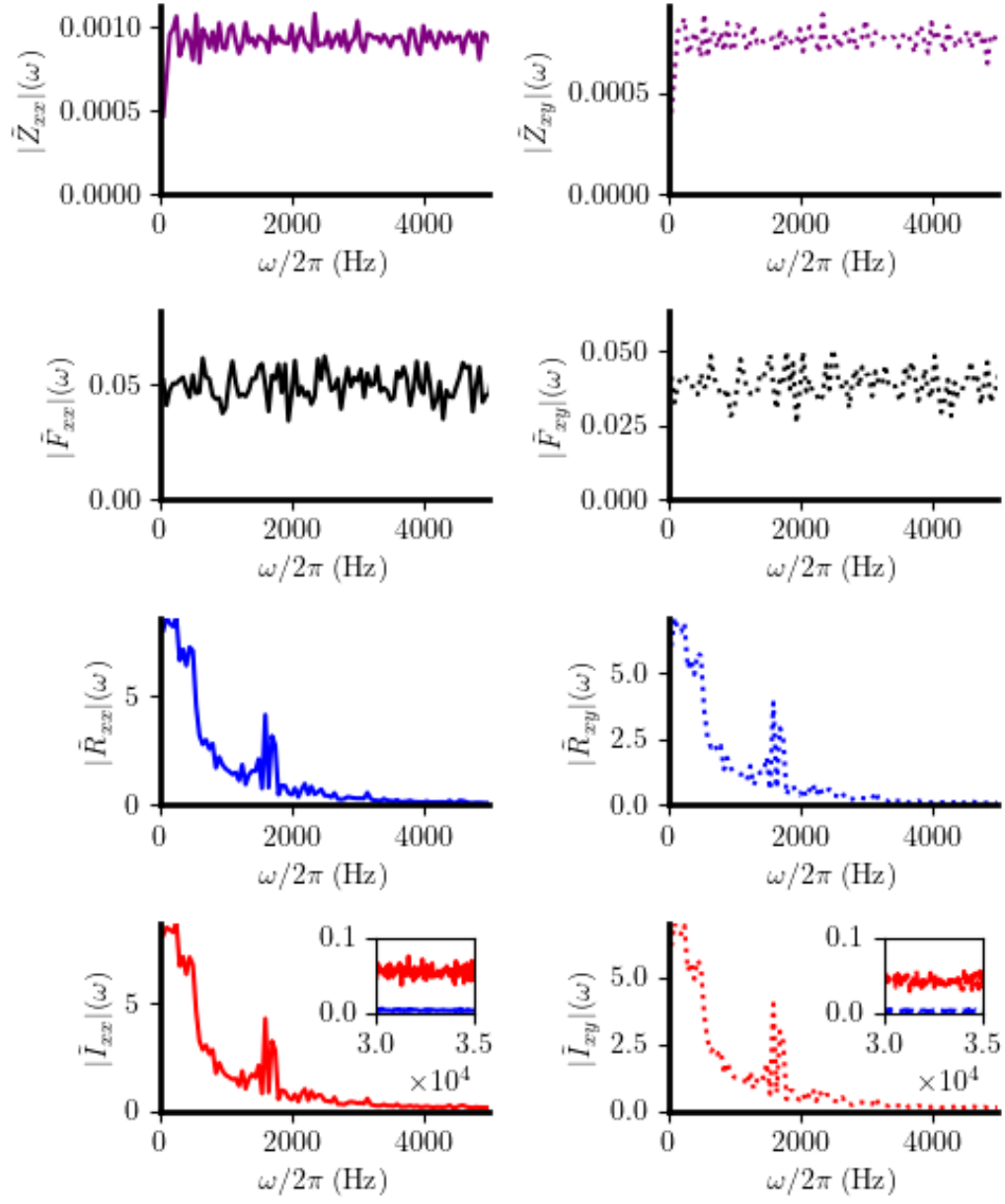


Figure 1.4

$$\Gamma_{ij}(|\Delta \mathbf{r}_{ij}|) = \gamma \cdot \exp \left( -\frac{1}{2} (\mathbf{r}_i - \mathbf{r}_j)^T \boldsymbol{\Sigma}_i (\mathbf{r}_i - \mathbf{r}_j) \right) \quad (1.23)$$

where  $\boldsymbol{\Sigma}_i = \sigma_i^2 I$  with the two-dimensional identity matrix  $I$ . The parameter  $\sigma_i$  can be



**Figure 1.5**

intepreted as the *reach* of a neuron  $i$ . Furthermore, for the kernel  $\Gamma_{ij}$  to represent a binomial probability at each point of its domain, we must have that

$$\Gamma_{ij}(|\Delta \mathbf{r}_{ij}|) \leq 1 \quad (1.24)$$

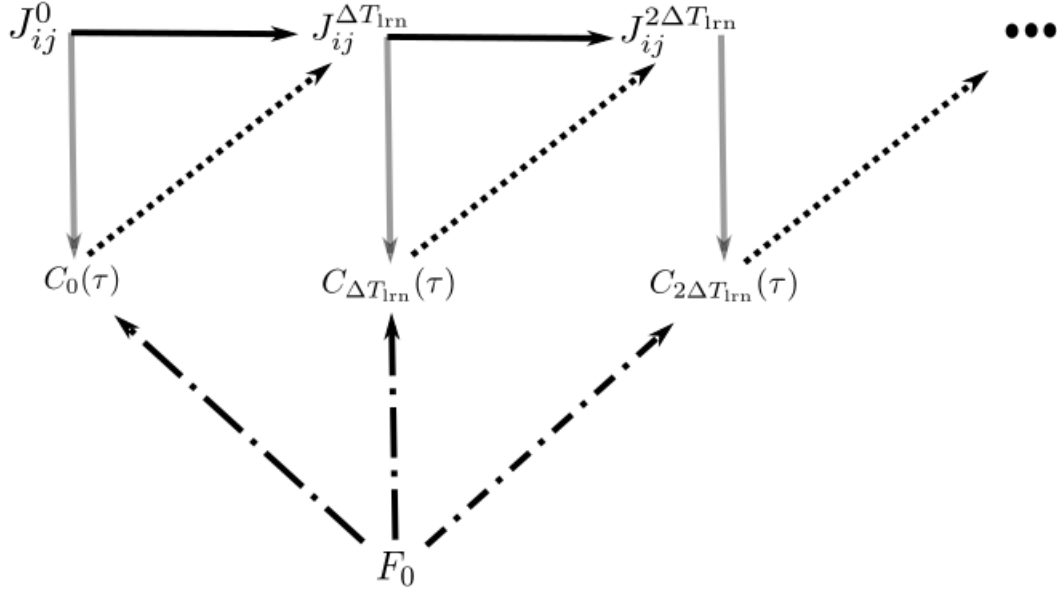


**Figure 1.6:** Computational graph describing the update of synaptic weights  $J_{ij}$  and the cross-covariance matrix  $C(\tau)$  over multiple stimulus periods of length  $\Delta T_{\text{stim}}$ . The learning period  $\Delta T_{\text{lrn}} \ll T_{\text{stim}}$  determines the frequency of learning updates within the period  $\Delta T_{\text{stim}}$

Plugging in our definition (3.5) gives the following inequality

$$\gamma \cdot \exp \left( -\frac{\min_j (|\Delta \mathbf{r}_{ij}|^2)}{2\sigma_i^2} \right) \leq 1$$

The largest possible value of the exponential is achieved at  $\min_j (|\Delta \mathbf{r}_{ij}|^2) = \Delta$  (a neighboring lattice point). Therefore,  $\gamma$  is upper bounded according to  $\gamma \leq \exp \left( \frac{\Delta^2}{2\sigma_i^2} \right)$ . For the remainder of our analysis we will fix  $\gamma = 1$  and focus our attention to the impact of the parameters  $\sigma$  and  $\Gamma_0$  on the statistics of connectivity.

As can be seen in Fig. (3.1a), when  $\Gamma_{ij} = \Gamma_{ji}$  we have that  $p_{ij} = p_{ji}$  for all  $|\Delta \mathbf{r}_{ij}|$ . We formally refer to this case as the *homogeneous gaussian network*. While this is not necessarily

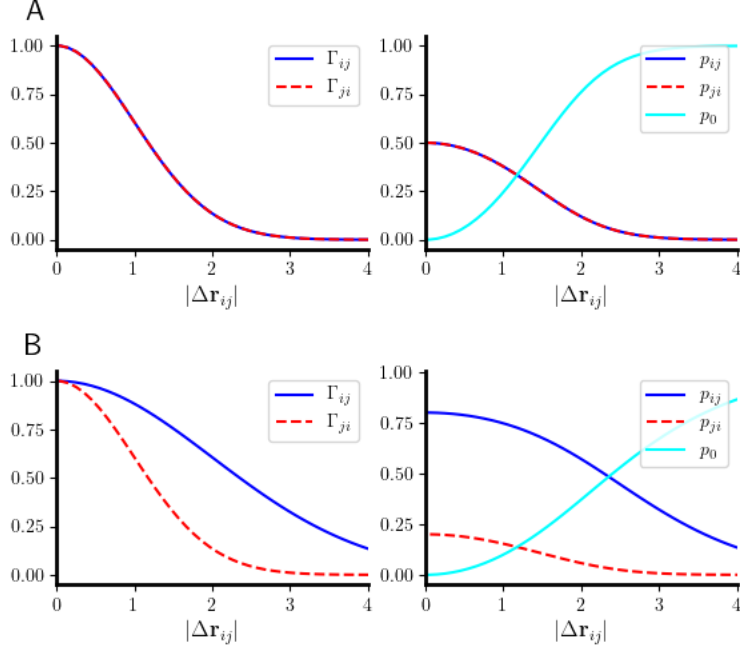


**Figure 1.7: Synapse probabilities for gaussian connectivity** (a) Binomial probabilities for two identical gaussian kernels ( $\sigma = 1$ ) separated by a distance  $|\Delta \mathbf{r}_{ij}|$  and the probability of no synapse  $\Gamma_0$  (left) and the corresponding multinomial probabilities (right). (b) Binomial probabilities for two different gaussian kernels ( $\sigma_1 = 1, \sigma_2 = 2$ ) separated by a distance  $|\Delta \mathbf{r}_{ij}|$  and the probability of no synapse  $\Gamma_0$  (left) and the corresponding multinomial probabilities (right).

a realistic case, it serves as a useful testbed for the graph theoretic concepts to be used in later analyses.

### 1.3.2 Homogeneous Gaussian networks

Let us now examine the statistics of the out-degree of a neuron  $i$  assuming that the connectivity parameter  $\sigma$  and  $\Gamma_0$  are homogeneous across the network i.e., they are constant for all neurons. Using Eq. (3.2), we have

$$\langle N_{ij} \rangle = \left( \frac{1 - \Gamma_0}{N} \right) \sum_j \Gamma_{ij} (1 - \Gamma_{ji}) \cdot Z_{ij}^{-1} \quad (1.25)$$

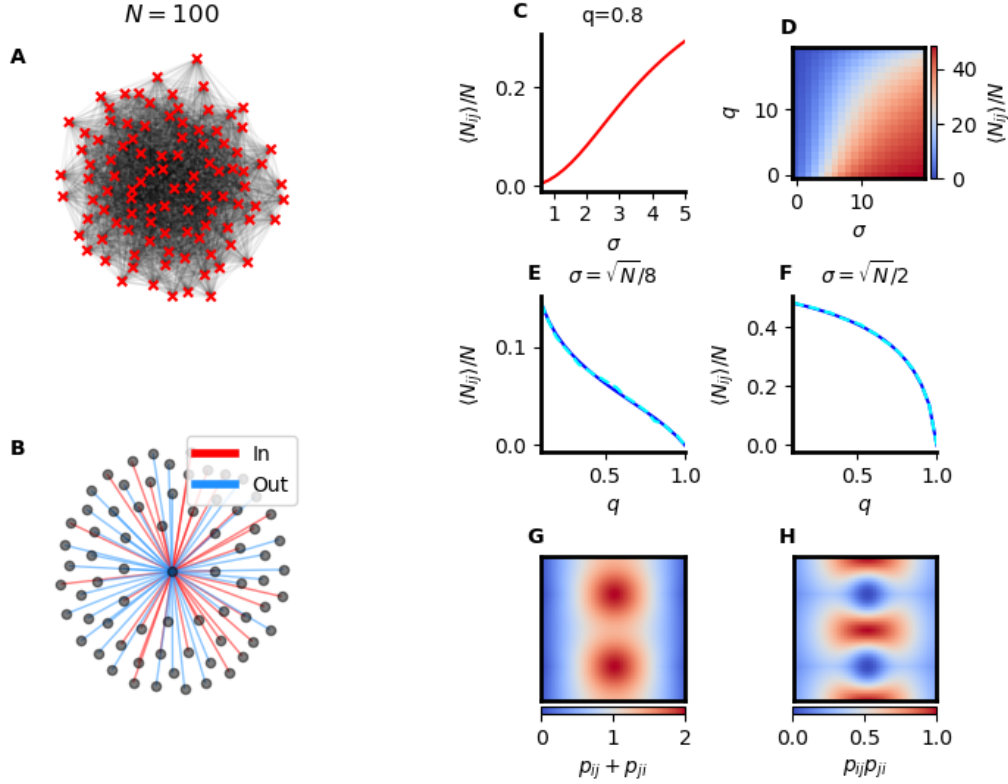


**Figure 1.8: The homogeneous Gaussian network.** (A) An example homogeneous network containing  $N = 100$  neurons. (B) An example neuron extracted from (A) with outgoing synapses labeled in blue and incoming synapses labeled in red. (C,D) The ratio  $\langle N_{ij} \rangle / N$  as a function parameters  $(\sigma, \Gamma_0)$  for a sparse network (C) and a network with variable sparsity (D). (E,F) The ratio  $\langle N_{ij} \rangle / N$  for fixed  $\sigma$  and variable sparsity. (G,H) Binomial probability maps for two nearby neurons expressed as a sum  $p_{ij} + p_{ji}$  and product  $p_{ij}p_{ji}$

a sum that can be carried out numerically. Interestingly, in the homogeneous case, the parameter  $\gamma$  and  $\Gamma_0$  become redundant. This can be seen by considering that multiplying  $p_{ij}$  and  $p_{ji}$  by the same constant factor  $\gamma$  is equivalent to the transformation  $\Gamma'_0 = 1 - \gamma(1 - \Gamma_0)$ .

In other words, for the homogeneous case, the multiplication by  $\gamma$  can be represented by a suitable selection of  $\Gamma_0$  and can be set  $\gamma = 1$ . Numerical evaluation of (3.7) shows that the ratio  $\langle N_{ij} \rangle$  increases monotonically for increasing  $\sigma$ , as expected from (3.1b) and saturates at  $\langle N_{ij} \rangle = 0.5$  at a rate proportional to  $\sigma$ . This can be understood from the fact that as

$\Gamma_0 \rightarrow 1$  we have  $p_0 \rightarrow 0$  and the multinomial distribution in (3.2) is reduced to a binomial distribution with  $p_{ij} = p_{ji} = 1/2$ .

Furthermore, in addition to the average degree of a neuron, we are interested in the average number of shared inputs (outputs) between two neurons. We expect that this statistic makes at least a partial contribution to pairwise correlations in the voltage dynamics between two cells. To address this, we consider the average number of shared connections  $\langle S_{ij} \rangle$  between a neuron  $i$  and  $j$  as a function of their distance  $|\Delta \mathbf{r}_{ij}|$ . In essence, this is the product  $p_{ik} \cdot p_{jk}$  for a third neuron  $k$  with  $i, j \neq k$ . The symmetry present in the homogeneous case allows us to perform this computation rather easily,

$$\langle S_{ij} \rangle = \frac{1}{N} \sum_k p_{ik} \cdot p_{jk} \quad (1.26)$$

$$= \frac{(1 - \Gamma_0)^2}{N} \sum_k \frac{\Gamma_{ik}(1 - \Gamma_{ki})\Gamma_{jk}(1 - \Gamma_{kj})}{Z_{ik}Z_{jk}} \quad (1.27)$$

which can be carried out numerically over the two-dimensions of space. Self-consistent with our definition of the connectivity kernel, the normalized number of shared connections decays with a gaussian profile for increasing  $|\Delta \mathbf{r}_{ij}|$  as can be seen in Fig. (3.3).

### 1.3.3 *Excitatory-inhibitory Gaussian networks*

Thus far we have considered only the case where the spatial connectivity kernel is the same for every neuron. However, the integrative properties of neurons depend strongly on the number, proportions and distribution of excitatory and inhibitory synaptic inputs they receive (Megias 2001). Also, the role excitatory-inhibitory balance in network dynamics has been a subject of recent debate. Indeed, balanced recurrent excitation and inhibition capture the irregular and asynchronous spiking activity with weak correlations reported in cortex. The spatial extent of excitation relative to inhibition has been shown to have a strong impact on network

dynamics. In particular, when the spatial extent of excitation is sufficiently smaller than inhibition, the balanced fixed point loses stability (Rosenbaum 2014).

To account for excitatory and inhibitory cell types within this framework, we must differentiate  $\langle N_{ij} \rangle$  for excitatory and inhibitory neurons and solving for both the mean in-degree and out-degree separately. Thus we have the quantities  $\langle E_E^{\text{out}} \rangle, \langle E_I^{\text{out}} \rangle, \langle E_I^{\text{in}} \rangle$  and  $\langle I_E^{\text{out}} \rangle, \langle I_I^{\text{out}} \rangle, \langle I_E^{\text{in}} \rangle$ . Under the assumption that excitatory and inhibitory neurons are distributed uniformly in two-dimensional space, we have that  $\langle E_I^{\text{out}} \rangle = \langle I_E^{\text{in}} \rangle$  and  $\langle E_I^{\text{in}} \rangle = \langle I_E^{\text{out}} \rangle$ . For brevity, we drop the superscripts and compute the above averages according the general prescription provided by (3.3). The result of these numerical calculations allow us to observe that, for  $\Gamma_0 = 0.2$ , the fraction of the target population saturated by excitatory or inhibitory outputs increases monotonically with  $\sigma_E$  and  $\sigma_I$  (Fig 3.4 b,d). The parameter maps provided in (Fig 3.4 b,d) are a starting point for our later discussions of newtork dynamics.



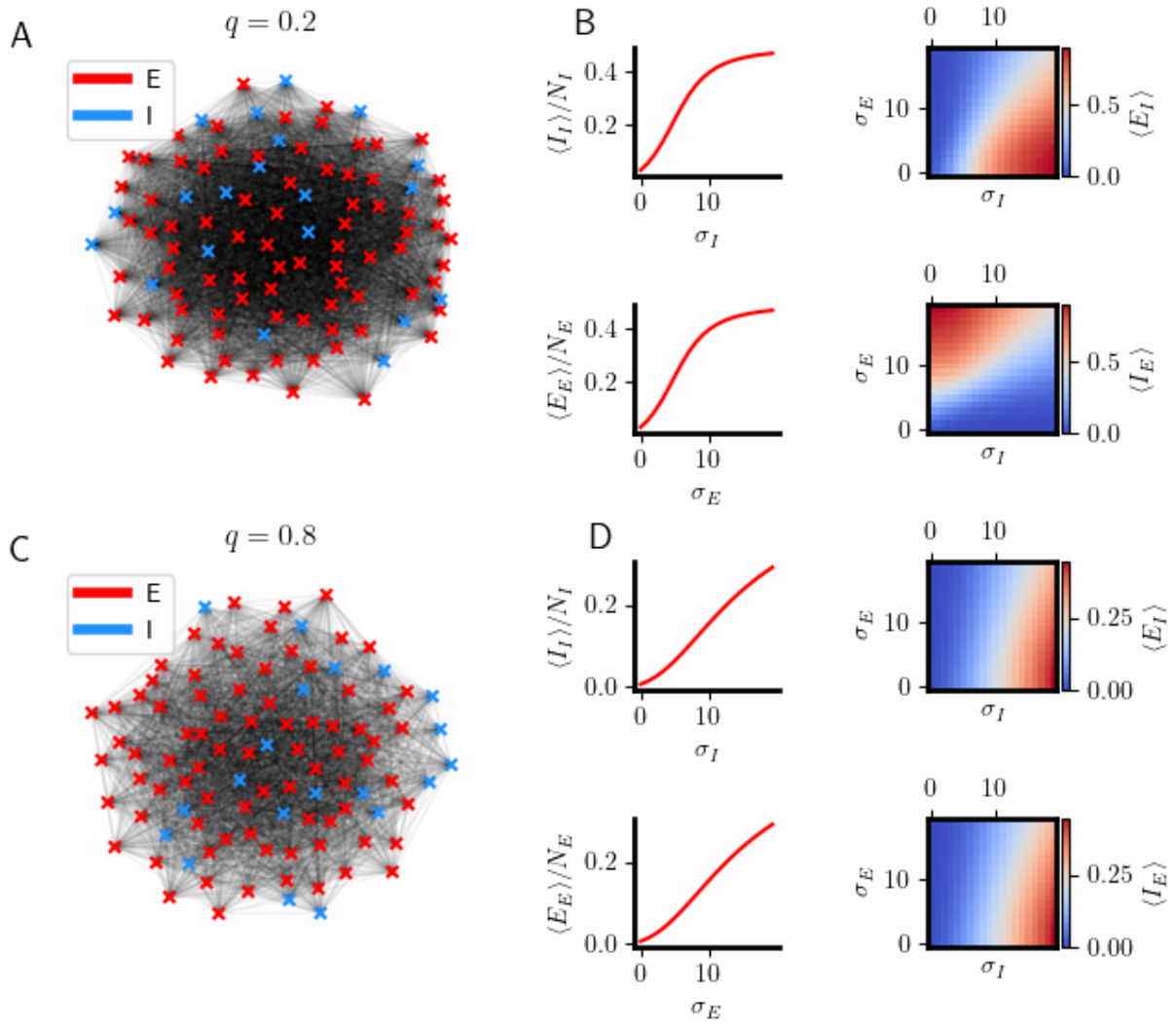


**Figure 1.9: Average degree in an excitatory-inhibitory network** (A) Schematic illustrating the notation used for excitatory-excitatory, excitatory-inhibitory, inhibitory-excitatory, and inhibitory-inhibitory synapses. (B) An example dense excitatory-inhibitory network ( $\Gamma_0 = 0.2$ ) and  $p_E = 0.8$ . (C) Average number of synapses in the dense network normalized to the target population size as a function of parameters  $\sigma_E$  and  $\sigma_I$ . (D) An example sparse excitatory-inhibitory network ( $\Gamma_0 = 0.8$ ) and  $p_E = 0.8$ . (E) Average number of synapses in the sparse network normalized to the target population size as a function of parameters  $\sigma_E$  and  $\sigma_I$ .

## 1.4 Methods

### 1.4.1 Signal processing techniques

The cross-correlation of discrete signals  $x(t)$  and  $y(t)$  is generally defined as the following convolution in the time-domain

$$R_{xy}(\tau) = x(t) * y(t) = \sum_{k=-\infty}^{\infty} x(t)y(t + \tau) \quad (1.28)$$

where the  $*$  symbol represents the convolution operation. Let  $\psi_x(\omega)$  be the discrete-time Fourier transform (DTFT) of  $x(t)$  i.e.,

$$\psi_x(\omega) = \sum_{t=-\infty}^{\infty} x(t) (\exp -i\omega t) \quad (1.29)$$

where an identical expression exists for  $\psi_y(\omega)$ . According to the convolution theorem, convolution in the time-domain is equivalent to multiplication in the frequency domain with one of the signals time-reversed. Therefore, we can write

$$\text{DTFT}[x(t) * y(t)](\omega) = \lim_{T \rightarrow \infty} \frac{1}{2\pi T} \psi_x^*(\omega) \psi_y(\omega) \quad (1.30)$$

Let  $S_{xy}(\omega) = \lim_{T \rightarrow \infty} \frac{1}{2\pi T} \psi_x^*(\omega) \psi_y(\omega)$ , which is commonly called the *cross spectral density* of signals  $x(t)$  and  $y(t)$ . This is simply the DTFT of the cross-correlation function meaning that  $R_{xx}(\tau)$  and  $S_{xx}(\omega)$  form a Fourier pair. This result provides us an efficient means of computing cross-correlations and autocorrelations of synaptic currents by multiplication in the frequency domain and taking the inverse discrete transform.

$$\mathbb{P} = \frac{p_n \prod_{m \neq n} (1 - p_m)}{\sum_n p_n \prod_{m \neq n} (1 - p_m)} = \frac{p_n \prod_{m \neq n} (1 - p_m)}{Z} \quad (1.31)$$

where  $Z$  is a normalization constant. For generating synapses, the probabilities of (3.1) are the probabilities over the possible synaptic states between  $i$  and  $j$

$$\mathbb{P} = \left\{ \begin{array}{l} p_{ij} = \Gamma_{ij}(1 - \Gamma_{ji})(1 - \Gamma_0) \cdot Z^{-1} \\ p_{ji} = \Gamma_{ji}(1 - \Gamma_{ij})(1 - \Gamma_0) \cdot Z^{-1} \\ p_0 = \Gamma_0(1 - \Gamma_{ij})(1 - \Gamma_{ji}) \cdot Z^{-1} \end{array} \right\} \quad (1.32)$$

$$Z = \Gamma_{ij}(1 - \Gamma_{ji})(1 - \Gamma_0) + \Gamma_{ji}(1 - \Gamma_{ij})(1 - \Gamma_0) + \Gamma_0(1 - \Gamma_{ij})(1 - \Gamma_{ji})$$

Sampling from the distribution  $\mathbb{P}$  for each of the  $N^2 - N$  possible synapses (excluding autapses), we can generate an asymmetric adjacency matrix  $\mathcal{C} \in \mathbb{F}_2^{N \times N}$ . An element  $\mathcal{C}_{ij} = 1$  defines a synapse from  $i \rightarrow j$  and  $\mathcal{C}_{ji} = 1$  defines a synapse from  $j \rightarrow i$ .

Defining the generation of network connectivity in this way proves useful upon the realization that the network can be described by binomial statistics, similar to the well-known Erdos-Renyi (ER) random graph. Graph theory provides a rich set of metrics that can be used to discuss the statistical properties of the network defined by  $\mathcal{C}$  and in turn the chosen kernel  $\Gamma$ . Assuming that we can compute the probabilities  $p_{ij}, p_{ji}$  and  $p_0$  for a particular  $\Gamma$  and every synapse is generated independently, the mean of the out-degree distribution is

$$\langle N_{ij} \rangle = \sum_j \Gamma_{ij}(1 - \Gamma_{ji})(1 - \Gamma_0) \cdot Z^{-1} \quad (1.33)$$

where the spatial dependence of the individual kernels is implied. The in-degree distribution is found by simply swapping  $i$  and  $j$ . The variance of the out-degree distribution is

then

$$\text{Var}(N_{ij}) = \sum_j \langle N_{ij}^2 \rangle - \langle N_{ij} \rangle^2 \quad (1.34)$$

$$= \sum_j \langle N_{ij} \rangle - \langle N_{ij} \rangle^2 \quad (1.35)$$

from the linearity of variance property. We will analyze the in-degree and out-degree distributions of a graph generated when the connectivity kernel is a symmetric Gaussian extending over two-dimensions. We refer to this case as a *two-dimensional gaussian network*.

The following model for generating the backbone for network of neurons rests on the assumption that we can create connectivity solely from pairwise connection probabilities. Let us define a spatial connectivity kernel  $\Gamma_i(\mathbf{r}_j)$  with  $i, j \in \{n\}_{n=1}^N$  which defines the binomial probability that a neuron  $i$  synapses onto a different cell  $j \neq i$  at spatial coordinate  $\mathbf{r}_j$ . Here, the function  $\Gamma_i(\mathbf{r})$  is not itself a probability distribution but rather represents one component of a distribution that is defined for each possible pairs  $i, j$  for a given  $i$ . That distribution is completely represented for a pair  $i, j$  with knowledge of the kernel  $\Gamma_j(\mathbf{r}_i)$  and an additional probability that no synapse occurs  $\Gamma_0$ . The parameter  $\Gamma_0$  will be referred to as the *sparsity parameter* throughout the remainder of the text. Together, these three binomial probabilities can be renormalized to form a multinomial distribution  $\mathbb{P}_{ij}$  at every possible synapse  $ij$ . A general definition of the multinomial distribution is

[1] D.O. Hebb *The organization of behavior: A neurophysiological theory*. John Wiley and Sons. 1949.